A Comparison of the Reactivity of Ni Atoms Toward CH_4, SiH_4, and SnH_4: A Combined Matrix Isolation and Quantum-Chemical Study

Hans-Jörg Himmel*[a]

Abstract: Nickel atoms are shown to react spontaneously with SiH_4 and SnH_4 to give the insertion products $HNiSiH_3$ and $HNiSnH_3$. With CH_4, however, no spontaneous reaction occurs, in agreement with earlier reports; $HNiCH_3$ can be formed only on photolytic activation of the Ni atom. The reaction products were characterized experimentally by IR spectroscopy, including the effect of isotopic substitution (H/D), and by quantum-chemical calculations. They all have C_s symmetry with a terminal Ni–H bond and three terminal E–H bonds (E = Si, Sn). Strikingly, the H-Ni-E bond angles are less than 90°, and there is a weak interaction between the H atom bound to Ni and the E atom. The structures are compared with those of other molecules of general formula $MSiH_4$ that have been characterized recently in our group (M = Ti, Ni, Ga). While $TiSiH_4$ has three Ti-H-Si bridges, both $NiSiH_4$ and $GaSiH_4$ exhibit only terminal Ni–H and E–H bonds, but with the difference that there is no interaction between the H atom bound to Ga and the Si atom.

Keywords: insertion · matrix isolation · nickel · reaction mechanisms · vibrational spectroscopy

Introduction

It has been shown that most transition-metal atoms, whether neutral or positively or negatively charged, do not undergo spontaneous (thermal) reaction with CH_4. Ni is no exception, and there is no sign of a spontaneous reaction between Ni atoms and CH_4 under the conditions of matrix isolation. In contrast to the atoms in their ground electronic state ($^3F_4$ with the configuration $[Ar]3d^84s^2$), photoactivated Ni atoms were reported to insert into the C–H bond to give $HNiCH_3$.[1] In these studies, the Ni atoms were excited with UV radiation from a mercury arc lamp ($\lambda_{max} = 254$ nm), which can cause excitation of one electron from the 4s into the 4p orbital (resulting in the y^3D^0, y^3F^0, or z^3G^0 electronic states), and also excitation of the second electron from the 4s into a 3d orbital (leading to the $z^3F_4^0$ or z^3D^0 electronic states). Theoretical estimates on the basis of DFT calculations predict the reaction between Ni and CH_4 to give $HNiCH_3$ to be exothermic by $-34.0\ kJ\,mol^{-1}$. According to the calculations, the reaction barrier is $+40.7\ kJ\,mol^{-1}$.[2] In an earlier study using the average coupled pair functional (ACPF) method, the reaction energy and barrier were calculated to be about -13.8 and $+74.9\ kJ\,mol^{-1}$, respectively.[3] Thus, if correlation effects are considered adequately, the reaction is calculated to be slightly exothermic by both DFT and ab initio methods [MRCI calculations predict the reaction to be slightly endothermic ($17.9\ kJ\,mol^{-1}$)].[3] Theoretical analysis of the origins of the barrier indicates that the $d^{n+1}s$ state of the metal atom is generally active in breaking the C–H bond.[3] Another factor is the ability of the metal to engage in sd hybridization, which depends on the orbital sizes: this is judged to be the main reason for the generally slightly smaller barrier for second-row transition metals in comparison with first-row transition metals.[3] Studies on the oxidative addition of CH_4 to ligand-bearing metal atoms, such as $[Pd(PH_3)_2]$ and $[Pt(PH_3)_2]$ and other phosphane complexes,[4] show that the ligand can have a significant influence on barrier height. Nevertheless, naked metal atoms were used as the first and smallest model systems for analyzing this kind of reaction.

Numerous studies on gaseous anionic or cationic metal atoms or clusters have also been reported. An example relevant to the present experiments and calculations is the reaction of Pt_n^+ clusters ($n = 1$–5) with CH_4, which leads spontaneously to $[Pt_nCH_2]^+$ and H_2.[5] Thus, in the gas phase, the reaction apparently cannot be halted at the step affording the insertion product HPt_nCH_3, but leads directly to dehydrogenation. One reason for the differences between the results of gas-phase and matrix-isolation studies arises from the ability of the matrix to act as a sink for the energy re-

[a] Dr. H.-J. Himmel
Institut für Anorganische Chemie
Universität Karlsruhe
Engesserstrasse, Geb. 30.45
76180 Karlsruhe (Germany)
E-mail: himmel@chemie.uni-karlsruhe.de

 DOI: 10.1002/chem.200305763

leased in the course of an exothermic reaction and to prevent the escape of all but the smallest fragments.

While CH_4 addition mechanisms have been studied in some depth with the help of small model systems, less attention has been paid to SiH_4 addition reactions. Industrially, C–H activation is certainly a more important process than Si–H activation. Nevertheless, much can be learnt by comparing oxidative addition of CH_4 and SiH_4. As expected, the reactivity of metal atoms toward SiH_4 is higher than toward CH_4, but there are large differences between the elements, which are worth studying in more depth. Previous investigations have provided a comparison of the reactivities of the main group elements Al and Ga and of the transition-metal Ti toward CH_4,[6,9] SiH_4,[7–9] and SnH_4.[9,10] These studies showed that matrix-isolated Al or Ga atoms react spontaneously to form a weakly bound complex $M{\cdot}SiH_4$ with η^2 coordination of SiH_4. Photolysis at $\lambda = 410$ or 254 nm is needed to convert this complex to the insertion product $HMSiH_3$, a bent radical with C_s symmetry. Interestingly, this product of oxidative addition can be converted almost reversibly back to the complex by photolysis at $\lambda = 580$ nm. Ti and Ni atoms also react spontaneously with SiH_4, but to a more marked degree. With Ti atoms this reaction gives the complex $Ti{\cdot}SiH_4$, *cis*- and *trans*-$HTi(\mu\text{-}H)_2SiH$ and, as the most stable product, $HTi(\mu\text{-}H)_3Si$.[9] The first three species can be converted to the last-named by selective photolysis. These results indicate that the reaction of Ti with SiH_4 to give $HTi(\mu\text{-}H)_3Si$ is subject to a small barrier. Another remarkable finding is that Ga_2 dimers are much more reactive than Ga atoms. We have shown previously that Ga_2 reacts spontaneously with SiH_4 to yield $HGa(\mu\text{-}SiH_3)Ga$.[8]

Here the reactivity of Ni atoms toward CH_4, SiH_4, and SnH_4 is compared by using the matrix-isolation technique. While the reaction with CH_4 was studied previously,[1] to our knowledge there is no published experimental study on the reactions with SiH_4 or SnH_4. The possible insertion product $HNiSiH_3$ was analyzed theoretically.[11] However, it will be shown here that the structure reported there is not the global energy minimum structure, but only a local minimum on the potential energy surface. This local minimum form might be better suited for simulating surface effects, as was the purpose of the earlier study, than the global energy minimum form. Finally, an experimental study on the adsorption of SiH_4 on Ni surfaces was reported.[12] Such studies demonstrate the need for a thorough investigation of the reaction between Ni atoms and SiH_4 on an experimental basis, the results of which will have wide significance with regard to both understanding and potential applications.

Experimental Section

Details of the matrix-isolation experiment are given elsewhere.[13] Ni was evaporated from a resistively heated Ni wire with a diameter of 0.5 mm (Goodfellow, 99.0%). A power of 45–50 W was used. The Ni content of the matrix was analyzed by UV/Vis spectroscopy.

SnH_4 and SnD_4 were synthesized from $SnCl_4$ (Aldrich, purified by distillation) and $LiAlH_4$ or $LiAlD_4$ in diglyme (purified by refluxing for 3 d over Na and distillation) and purified by fractional condensation in vacuo. SiH_4 was used as delivered (Linde, $>99.99\%$). SiD_4 was made from $SiCl_4$ and $LiAlD_4$ in diglyme and purified by fractional condensation in vacuo. Ar was used as delivered from Messer (99.998%).

The IR spectra were recorded with a Bruker 113v FTIR spectrometer equipped with a liquid-N_2-cooled MCT detector for measurements in the spectral range 4000–650 cm^{-1}, a DTGS detector for measurements in the region 700–200 cm^{-1}, and a liquid-He-cooled Bolometer in the region 700–30 cm^{-1} (not used in this study). A resolution of 0.2 cm^{-1} was chosen.

The UV/Vis spectra were measured with an Xe arc lamp (Oriel), an Oriel Multispec spectrograph, and a photodiode array detector. The resolution was varied from 0.2 to 0.5 nm.

Photolysis was performed with a medium-pressure Hg lamp (Philips LP 125) operating at 100 W. The radiation was transmitted through a water filter to protect the matrix from IR light. Interference filters were used for selective photolysis.

Quantum-chemical calculations were performed with the the TURBOMOLE program.[14] The BP and B3LYP functionals were used in combination with SV(P) and TZVPP basis sets.

Results

$Ni + CH_4$: The IR spectrum recorded on deposition of Ni atoms with CH_4 in an Ar matrix did not show any absorptions attributable to a product of the reaction between Ni atoms and CH_4. The spectrum contained, besides the strong bands due to CH_4, an absorption at 2089.8 cm^{-1} and an extremely weak band at 564.2 cm^{-1}, both of which can be assigned to NiNN, formed by reaction between Ni atoms and traces of N_2.[15] In some experiments, the spectrum also contained an extremely weak band at 1994.4 cm^{-1} for the monocarbonyl NiCO.[16] It can be concluded that Ni atoms in their ground electronic state do not react spontaneously with CH_4, in agreement with a previous study on this system.[1] On UV photolysis ($\lambda_{max} = 254$ nm), a weak absorption grew at 1945.2 cm^{-1}, as was observed previously and assigned to the ν(Ni–H) stretching mode of the insertion product $HNiCH_3$. The present results are thus in line with those obtained previously.[1] In summary, photolysis is needed to bring about the insertion of the Ni atom into a C–H bond of CH_4. Even with photoactivated Ni atoms, however, the product yield appears to be low. Prolonged photolysis caused the absorptions due to $HNiCH_3$ first to increase and then slowly to decrease.

$Ni + SiH_4$: The IR spectrum recorded immediately on deposition of Ni atoms with SiH_4 in an excess of Ar (1% SiH_4) is shown in Figure 1a. Strong and sharp absorptions at 2121.3, 2096.4, and 2024.1 cm^{-1} are evident. An additional strong band appears around 945 cm^{-1}, and several maxima at 948.6, 946.3, 944.0, and 941.1 cm^{-1} (see below). Finally, the spectrum contained evidence of weaker bands at 859.4, 505.6, and 353.8 cm^{-1}. Experiments with different concentrations of SiH_4 and/or Ni atoms in the matrix showed that all seven bands belong to the same common absorber, which is a spontaneously formed product of the reaction between Ni atoms and SiH_4. The matrix was then subjected to 30 min of photolysis with broad-band UV/Vis light ($200 \le \lambda \le 800$ nm). The IR spectrum recorded after this treatment is shown in Figure 1b. The bands due to the spontaneously formed product of the reaction between Ni and SiH_4 have decreased

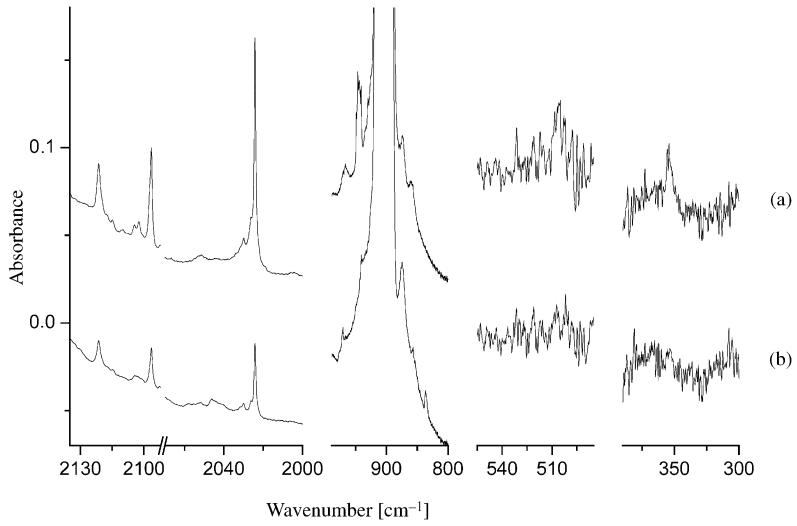

Figure 1. IR spectra obtained for the reaction of Ni atoms with SiH_4 (1%) in a solid Ar matrix at 12 K. a) On deposition. b) After 30 min of broad-band UV/Vis photolysis ($200 \leq \lambda \leq 800$ nm).

significantly. However, the spectrum failed to give evidence for any distinct decomposition product.

Figure 2 shows the corresponding IR spectra taken for an experiment with 1.5% SiH_4 in the matrix. The product bands in the spectrum recorded on deposition are significantly more intense (Figure 2a) than in the experiments with the lower SiH_4 concentration. In particular, the product bands in the region 600–200 cm^{-1} are now more clearly visible. The matrix was subjected to several cycles of selected photolysis. Photolysis for 15 min at $\lambda = 700$ nm had virtually no effect on the intensities of the bands. Photolysis at $\lambda =$ 410 nm for 30 min brought about some decrease in the band intensities. However, photolysis with broad-band visible light ($\lambda > 400$ nm) had a marked effect. The spectrum obtained after 20 min of such photolysis is shown in Figure 2b. The significant decrease in the product bands shows that this species has an electronic transition in the visible region. NiNN and NiCO are much more photosensitive than the product of the reaction between Ni and SiH_4. It can be seen from Figure 2 that the bands due to these two impurities can be virtually extinguished by short-term exposure to visible light. Figure 2c shows the spectrum measured after 20 min of broad-band UV/Vis photolysis ($200 \leq \lambda \leq 800$ nm). As expected, the bands again suffered a loss in intensity. As in previous experiments, little information on possible decomposition products can be gained from the spectra. There is only a weak band appearing at 433.6 cm^{-1} on photolysis with visible light and decaying on photolysis with broad-band UV/Vis light. The high-resolution IR spectra of the absorption around 945 cm^{-1} (Figure 3) clearly shows maxima at 948.6, 946.3, 944.0, and 941.1 cm^{-1}, the relative intensities of which changed during the photolysis cycles. Although all the components decreased on photolysis, the feature at 941.1 cm^{-1} appeared to decay less than the others. It is not clear whether this multiplet structure can be explained by the presence of more than one conformer of the molecule in the matrix host or by the occupancy of more than one type of matrix site.

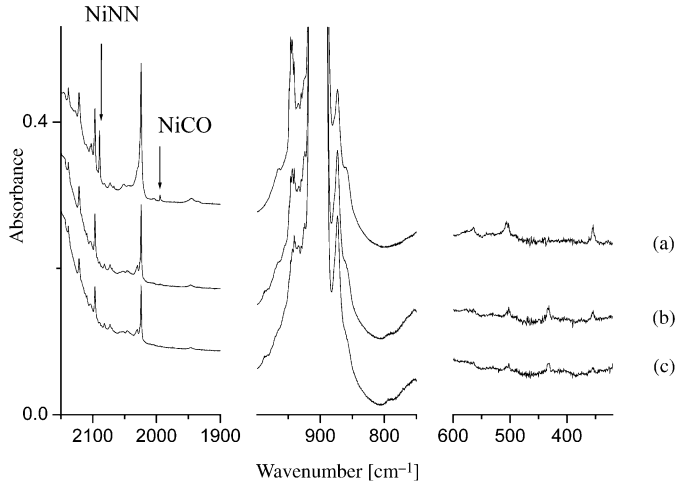

Figure 2. IR spectra obtained for the reaction of Ni atoms with SiH_4 (1.5%) in a solid Ar matrix at 12 K. a) On deposition. b) After 10 min of broad-band visible photolysis ($400 \leq \lambda \leq 800$ nm). c) After 30 min of broad-band UV/Vis photolysis ($200 \leq \lambda \leq 800$ nm).

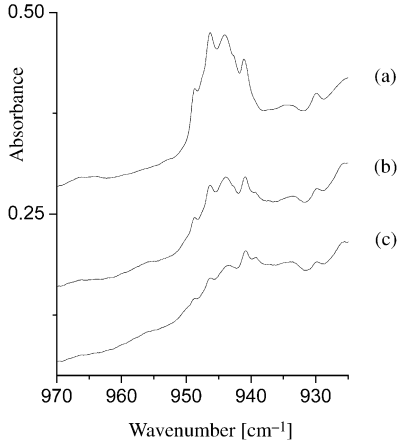

Figure 3. High-resolution IR spectrum showing the absorption around 945 cm^{-1}. a) On deposition. b) After broad-band visible photolysis ($400 \leq \lambda \leq 800$ nm). c) After broad-band UV/Vis photolysis ($200 \leq \lambda \leq 800$ nm).

The experiment was repeated with SiD_4 in place of SiH_4. Figure 4a shows the IR spectrum recorded on deposition. As with the experiments with SiH_4, absorptions attributable to a single product of the reaction between Ni and SiD_4 could already be observed at this stage. All the absorptions

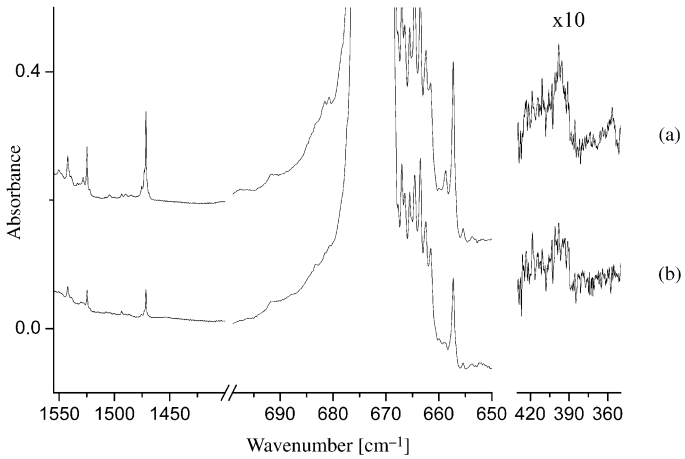

Figure 4. IR spectra obtained for the reaction of Ni atoms with SiD_4 in a solid Ar matrix at 12 K. a) On deposition. b) After 10 min of broad-band UV/Vis photolysis ($200 \leq \lambda \leq 800$ nm).

were red-shifted with respect to their H counterparts. Thus, the three intense absorptions at 2121.3, 2096.4, and 2024.1 cm^{-1} in the experiment with SiH_4 now occur at 1541.9, 1525.1, and 1471.7 cm^{-1}, respectively. The respective $\nu(H)/\nu(D)$ ratios are 1.3758:1, 1.3731:1, and 1.3753:1. These values indicate that the corresponding modes involve mainly the movement of H or D atoms attached to Si or Ni. Another band appeared at 657.3 cm^{-1}, close to the strong $\delta(SiD_3)$ deformation of SiD_4. The H counterpart of this band was presumably obscured by the corresponding SiH_4 absorption. Finally, a very weak feature at 398.5 cm^{-1} in the spectra for experiments with SiD_4 might be the D version of the band at 505.6 cm^{-1} in the experiments with SiH_4. The effects of photolysis were similar to those observed in the experiments with SiH_4. Thus, 30 min of photolysis decreased the product bands (see Figure 4b).

UV/Vis spectroscopy was employed to obtain further information. The UV/Vis spectrum of Ni atoms isolated in an Ar matrix in the absence of SiH_4 is shown in Figure 5a. The bands are in good agreement with those reported previously for Ni atoms isolated in an Ar matrix.[17,18] The intense bands with maxima at 312, 325, and 336 nm may be assignable to excitations from the $^3F_4$ ground electronic state to the excited z^3G^0, z^3D^0, or $z^3F_4^0$ electronic states, respectively. Figure 5b shows the UV/Vis spectrum of a matrix containing Ni vapor and SiH_4. This displays weaker bands due to atomic transitions. A broad band or background centered at roughly 400 nm might be associated with the reaction product of Ni and SiH_4. This broad band decreased slowly on photolysis, while the features due to the Ni atoms did not gain in intensity. It is thus unclear whether photodecomposition of the product leads back to Ni and SiH_4.

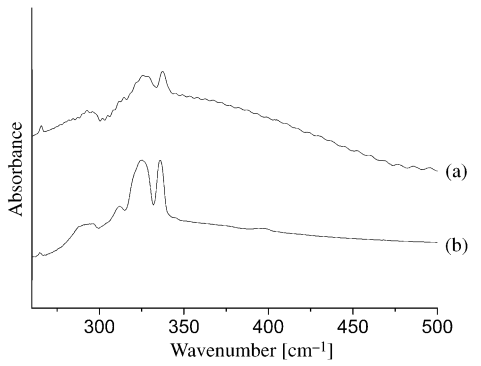

Figure 5. a) UV/Vis spectrum of Ni atoms isolated in an Ar matrix. b) UV/Vis spectrum of Ni atoms and 2% SiH_4 isolated in an Ar matrix at 12 K.

Ni + SnH_4: Figure 6a displays the IR spectrum recorded immediately on deposition of Ni vapor together with 0.1% SnH_4 in Ar at 12 K. It contained, in addition to the intense absorptions due to SnH_4, very strong bands at 1840.1, 1809.5, and 1749.8 cm^{-1}, and weaker features at 722.5, 709.7, and 652.9 cm^{-1}. In addition, two very weak absorptions were detected at 413.5 and 385.2 cm^{-1}. A weak feature also appeared at 2179.4 cm^{-1}. Experiments with different concentrations of SnH_4 and/or Ni in the matrix indicated that all the bands again belong to the same absorber. Thus, Ni also reacts spontaneously with SnH_4 to give a single product. The bands at 1840.1, 1809.5, and 1749.8 cm^{-1} appear in a region characteristic of modes with a high contribution from Sn–H stretching, whereas the feature at 652.9 cm^{-1} appears in a region characteristic of $\delta_{sym}(SnH_3)$ vibrations. The similarity of the IR spectra indicates that the products of the reactions of Ni atoms with SiH_4 and SnH_4 have similar structures. The matrix was subsequently subjected to 10 min of broad-band UV/Vis photolysis ($200 \leq \lambda \leq 800$ nm). This brought about complete extinction of the bands of the reaction product (Figure 6b). The Ni/SnH_4 reaction product is thus much more photosensitive than the Ni/SiH_4 product. The electronic transition responsible for the decomposition of the Ni/SnH_4 product also seems to lie in the visible region, as indicated by experiments with different photolysis conditions.

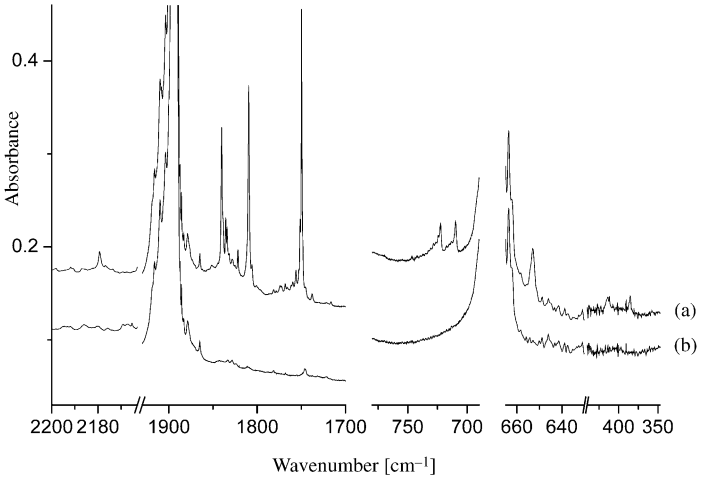

Figure 6. IR spectra obtained for the reaction of Ni atoms with SnH_4 in a solid Ar matrix at 12 K. a) On deposition. b) After 10 min of broad-band UV/Vis photolysis ($200 \leq \lambda \leq 800$ nm).

The experiment was repeated with SnD_4. As in the experiment with SnH_4, intense product bands could be detected immediately on deposition of Ni vapor together with SnD_4 (Figure 7). Eight bands of this product were identified. The very intense absorptions at 1840.1, 1809.5, and 1749.8 cm^{-1} in the spectrum with SnH_4 were shifted to 1321.4, 1300.7, and 1257.8 cm^{-1} with ν(H)/ν(D) ratios of 1.3925:1, 1.3912:1, and 1.3912:1, respectively. The large ν(H)/ν(D) ratios lend strong support to the assignment of the modes to vibrations with a large contribution from Sn–H stretching motions.[19] The two bands of roughly equal intensity at 722.5 and 709.7 cm^{-1} observed in the experiments with SnH_4 now appeared at 517.6 and 509.7 cm^{-1}, whereas the band at 652.9 cm^{-1} experienced a red shift to 469.0 cm^{-1}. Finally, two weak absorptions were detected at 300.3 and 282.9 cm^{-1}, which are probably the D counterparts of the bands at 413.5 and 385.2 cm^{-1} in the SnH_4 experiments.

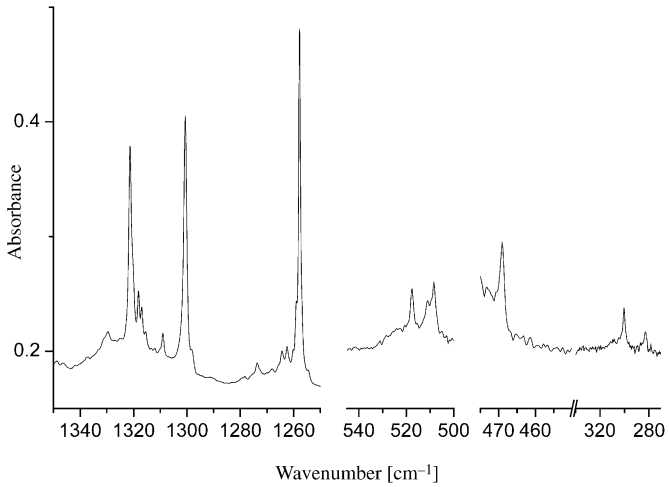

Figure 7. Difference between the IR spectra obtained before and after 10 min of broad-band UV/Vis photolysis ($200 \leq \lambda \leq 800$ nm) of an Ar matrix containing Ni atoms and SnD_4.

Discussion

The experiments described above show that Ni atoms react spontaneously with SiH_4 and SnH_4, but not with CH_4. The IR spectrum of the product of the reaction between Ni atoms and SiH_4 shows all the hallmarks of a species containing an SiH_3 group. The obvious inference is that this species is the insertion product $HNiSiH_3$. Likewise, the reaction with SnH_4 appears to lead to the insertion product $HNiSnH_3$. Quantum-chemical calculations with the BP and the B3LYP functionals were performed to gain information on possible structures of these two species, and the results are summarized in Tables 1 and 2. Both the choice of functional and the size of the basis set influence some of the structural details, generally to a small extent. Both $HNiSiH_3$ and $HNiSnH_3$ have C_s symmetry ($^1A'$ electronic ground state) with one terminal Ni–H bond and three terminal Si–H or Sn–H bonds. The most surprising feature is that the H-Ni-Si and H-Ni-Sn angles are slightly smaller than 90°. The distance between the H atom attached to the Ni atom and the Si or Sn atom is shorter than the sum of the van der Waals radii of H and Si or Sn (ca. 350 and 360 pm, respectively). This points to a weak interaction between the two atoms in the insertion product. More sophisticated quantum-chemical calculations are needed to analyze such an interaction.

In a previous theoretical study on $HNiSiH_3$, the molecule was predicted to have a linear H-Ni-Si skeleton conforming to C_{3v} symmetry.[11] Although the level of theory is not wholly satisfactory for calculating energy differences, our calculations indicate that the C_{3v}-symmetric form is not the global energy minimum geometry, but defines only a local minimum on the potential energy surface. According to our calculations, the C_s-symmetric form is energetically favored by 145.8 kJ mol^{-1} at the BP level and by 203.8 kJ mol^{-1} at the B3LYP level. The Ni–H bond in the C_{3v}-symmetric form is much longer than that of the C_s-symmetric form (156.6 and 144.1 pm, respectively). The value calculated here for the C_{3v}-symmetric form is in good agreement with that calculated previously (157.7 pm, CI method). Consequently, the mode with the highest contribution from the ν(Ni–H) motion is predicted to have a wavenumber of 1704 cm^{-1} for the C_{3v}-symmetric molecule, but 2033 cm^{-1} for the C_s-symmetric molecule. The C_s geometry calculated here for $HNiSiH_3$ is close to that found previously for $HNiCH_3$, for

Table 1. Calculated bond lengths [pm] and angles [°], wavenumbers [cm^{-1}] (intensities [km mol^{-1}] in parentheses), and zero-point vibrational energies (ZPVE) [kJ mol^{-1}] for $HNiSiH_3$ (C_s symmetry).

	BP/SV(P)	BP/TZVPP	B3LYP/SV(P)	B3LYP/TZVPP
Ni–H	144.1	142.5	143.9	142.1
Si–H	151.7, 151.7, 153.0	150.2, 150.2, 151.6	150.4, 150.4, 151.6,	149.0, 149.0, 150.3
Si···H	227.3	223.7	243.7	238.3
Ni–Si	210.8	212.8	214.8	215.8
H-Ni-Si	77.1	75.2	83.1	80.6
$\nu_1(a')$	2122.7 (114)	2123.1 (96)	2196.9 (108)	2189.7 (93)
$\nu_2(a')$	2053.6 (141)	2091.9 (33)	2132.4 (143)	2122.5 (152)
$\nu_3(a')$	2032.6 (4)	2048.2 (75)	2050.8 (66)	2095.0 (19)
$\nu_4(a')$	881.2 (50)	907.4 (46)	924.3 (58)	947.7 (53)
$\nu_5(a')$	875.5 (321)	848.2 (286)	902.7 (362)	886.5 (321)
$\nu_6(a')$	497.3 (16)	478.9 (11)	532.3 (47)	566.6 (74)
$\nu_7(a')$	398.2 (56)	401.9 (66)	387.5 (36)	454.3 (21)
$\nu_8(a')$	381.1 (2)	369.9 (3)	345.3 (17)	350.9 (3)
$\nu_9(a'')$	2119.1 (123)	2128.6 (104)	2197.6 (131)	2191.9 (115)
$\nu_{10}(a'')$	864.3 (36)	884.9 (32)	916.1 (49)	935.2 (43)
$\nu_{11}(a'')$	498.1 (4)	497.1 (6)	490.2 (4)	506.0 (6)
$\nu_{12}(a'')$	210.3 (19)	181.9 (21)	218.5 (30)	281.1 (28)
ZPVE	77.4	77.5	79.5	80.9

Table 2. Calculated bond lengths [pm] and angles [°], wavenumbers [cm^{-1}] (intensities [$km\,mol^{-1}$] in parentheses), and zero-point vibrational energies (ZPVE) [$kJ\,mol^{-1}$] for $HNiSnH_3$ (C_s symmetry).

	BP/SV(P)	BP/TZVPP[a]	B3LYP/SV(P)	B3LYP/TZVPP[a]
Ni–H	144.4	142.5	144.3	140.9
Sn–H	175.6, 175.6, 177.1	174.7, 174.7, 176.3	174.2, 174.2, 175.5	173.4, 173.4, 174.7
Sn···H	258.5	256.5	273.8	273.0
Ni–Sn	240.1	242.7	243.4	243.0
H-Ni-Sn	80.3	78.8	85.8	86.4
$\nu_1(a')$	2008.4 (50)	2072.3 (38)	2040.7 (95)	2168.0 (83)
$\nu_2(a')$	1764.6 (191)	1750.8 (172)	1828.6 (176)	1807.4 (187)
$\nu_3(a')$	1705.6 (214)	1692.1 (195)	1776.9 (248)	1757.8 (245)
$\nu_4(a')$	681.4 (48)	683.1 (49)	715.2 (53)	713.5 (54)
$\nu_5(a')$	648.0 (318)	648.9 (292)	679.1 (359)	674.1 (361)
$\nu_6(a')$	494.0 (56)	484.1 (64)	498.2 (81)	601.2 (97)
$\nu_7(a')$	317.4 (11)	328.7 (12)	329.1 (12)	320.6 (11)
$\nu_8(a')$	246.9 (2)	239.4 (3)	229.1 (3)	235.5 (2)
$\nu_9(a'')$	1754.9 (253)	1751.6 (247)	1819.8 (269)	1806.9 (284)
$\nu_{10}(a'')$	666.0 (39)	667.0 (43)	706.2 (52)	705.3 (54)
$\nu_{11}(a'')$	344.0 (9)	361.0 (11)	363.3 (23)	350.0 (15)
$\nu_{12}(a'')$	153.2 (22)	155.3 (24)	340.8 (18)	311.6 (30)
ZPVE	64.5	64.8	67.8	68.8

[a] TZVPP basis set for the H atoms and the Ni atom.

which Ni–H and Ni–C bond lengths of 147 and 198 pm and a H-Ni-C bond angle of 94° were calculated.[3]

Tables 3 and 4 compare the calculated [BP/SV(P)] and experimental vibrational properties of the H and D versions of the insertion products. An approximate description of the

Table 3. Comparison of the wavenumbers [cm^{-1}] (intensities [$km\,mol^{-1}$] in parentheses) observed and calculated [BP/SV(P)] for $HNiSiH_3$ and $DNiSiD_3$.

$HNiSiH_3$		$DNiSiD_3$		Assignment	Approx.
obsd	calcd	obsd	calcd		molec. motion
2096.4	2122.7 (114)	1525.1	1526.8 (70)	$\nu_1(a')$	ν_{sym}(Si–H)
2024.1	2053.6 (141)	1471.7	1476.2 (70)	$\nu_2(a')$	ν_{sym}(Si–H) [+ ν(Ni-H)]
–[a]	2032.6 (4)	–[a]	1455.6 (6)	$\nu_3(a')$	ν(Ni–H) [+ν_{sym}(Si–H)]
945	881.2 (50)	–[a]	634.3 (25)	$\nu_4(a')$	δ(SiH_3)
–[a]	875.5 (321)	657.3	652.6 (179)	$\nu_5(a')$	δ_{sym}(SiH_3)
505.6	497.3 (16)	398.5	418.8 (4)	$\nu_6(a')$	ν(Ni–Si) [+δ(Si-Ni-H)]
353.8	398.2 (56)	–[a]	284.9 (27)	$\nu_7(a')$	δ(Si-Ni-H)
–[a]	381.1 (2)	–[a]	324.8 (6)	$\nu_8(a')$	
2121.3	2119.1 (123)	1541.9	1534.9 (65)	$\nu_9(a'')$	ν_{as}(Si–H)
859.4	864.3 (36)	–[a]	621.0 (18)	$\nu_{10}(a'')$	
–[a]	498.1 (4)	–[a]	370.8 (1)	$\nu_{11}(a'')$	
–[a]	210.3 (19)	–[a]	150.2 (10)	$\nu_{12}(a'')$	

[a] Too weak to be observed or hidden by silane absorptions.

molecular motions for some of the modes is also included in the tables. Clearly, the degree of mode coupling is significant. This coupling is strong, for example, for the ν(Si–H) and ν(Ni–H) stretching modes in the a′ symmetry block for $HNiSiH_3$, which are very close in energy. As revealed in Tables 1 and 2, there are some differences in the vibrational properties—both wavenumbers and intensities–-between the results of the different methods of calculation. Nevertheless, the generally satisfying level of agreement lends persuasive support to the proposed assignments.

High-level ab initio quantum-chemical calculations are underway to secure more detailed information on the structures of the insertion product and the reaction mechanisms. The aim of future calculations is also to compare the mechanisms of the reactions of Ga and Ni atoms with SiH_4. The experiments showed that while the barrier is too high for spontaneous reaction in the case of the Ga atom,[8] the barrier must be near to zero for the Ni atom. A possible reason for the difference is that the metal atom has to change its electronic state in the course of the reaction. This requires less energy for Ni than for Ga. On the other hand, we have shown that Ga_2 is capable of inserting spontaneously into

Table 4. Comparison of the wavenumbers [cm^{-1}] (intensities [$km\,mol^{-1}$] in parentheses) observed and calculated [BP/SV(P)] for $HNiSnH_3$ and $DNiSnD_3$.

$HNiSnH_3$		$DNiSnD_3$		Assignment	Approx.
obsd	calcd	obsd	calcd		molec. motion
(2179.4)	2008.4 (50)	–[a]	1437.6 (26)	$\nu_1(a')$	ν(Ni–H)
1840.1	1764.6 (191)	1321.4	1256.0 (101)	$\nu_2(a')$	ν_{sym}(Sn–H)
1749.8	1705.6 (214)	1257.8	1215.1 (108)	$\nu_3(a')$	ν_{sym}(Sn–H)
722.5	681.4 (48)	517.6	485.6 (24)	$\nu_4(a')$	δ(SnH_3)
652.9	648.0 (318)	469.0	464.5 (165)	$\nu_5(a')$	δ_{sym}(SnH_3)
–[a]	494.0 (56)	–[a]	360.7 (26)	$\nu_6(a')$	ν(Ni–Sn) [+δ(Sn-Ni-H)]
385.2	317.4 (11)	300.3	246.8 (6)	$\nu_7(a')$	δ(Sn-Ni-H)
–[a]	246.9 (2)	–[a]	224.0 (3)	$\nu_8(a')$	
1809.5	1754.9 (253)	1300.7	1251.9 (130)	$\nu_9(a'')$	ν_{as}(Sn–H)
709.7	666.0 (39)	509.7	474.4 (20)	$\nu_{10}(a'')$	
413.5	344.0 (9)	282.9	248.9 (4)	$\nu_{11}(a'')$	
–[a]	153.2 (22)	–[a]	109.5 (12)	$\nu_{12}(a'')$	

[a] Too weak to be observed or hidden by stannane absorptions.

an Si–H bond of SiH_4,[8] and that Ga_2, but not Ga, reacts spontaneously with H_2.[20,21] The reason for these differences in reactivity is that the energy required to excite Ga_2 is much lower than that required to excite a Ga atom.[22]

The reaction of Ni atoms with CH_4 is slightly exothermic. According to a previous DFT estimates, the reaction energy is $-34.0\,kJ\,mol^{-1}$;[2] according to an ACPF estimate, the energy is $-13.8\,kJ\,mol^{-1}$.[3] Thus, the reactions of Ni atoms with SiH_4 and SnH_4 are also expected to be exothermic. A detailed analysis of the energies is the topic of ongoing research in our group.

Conclusion

The experiments and calculations described here sought to compare the reactivity of Ni atoms toward CH_4, SiH_4, and SnH_4. The reactions were studied by the matrix-isolation

technique. Ni vapor was co-condensed together with CH_4, SiH_4, or SnH_4 in an excess of Ar on a freshly polished copper block at 12 K, and the resulting Ar matrix was analyzed. The reaction products were identified experimentally by IR spectroscopy, including the effect of isotopic substitution, and by UV/Vis spectroscopy. The experimental results were supplemented by quantum-chemical calculations. It was found that Ni reacts spontaneously at 12 K with SiH_4 and SnH_4 to give the insertion products $HNiSiH_3$ and $HNiSnH_3$, respectively. With CH_4, on the other hand, spontaneous reaction does not occur, and the Ni atoms must be electronically excited to induce insertion into a C–H bond. The products $HNiSiH_3$ and $HNiSnH_3$ exhibit only terminal Ni–H, Si–H, and Sn–H bonds. Intriguingly, the H-Ni-Si and H-Ni-Sn angles are smaller than 90°, and the fact that the H···Si and H···Sn distances are significantly shorter than the sums of the respective van der Waals radii indicates some degree of interaction.

Figure 8 compares the structures of the products of the reactions of SiH_4 with Ti, Ni, and Ga (M) atoms, which in each case give a product of formula $MSiH_4$. However, the

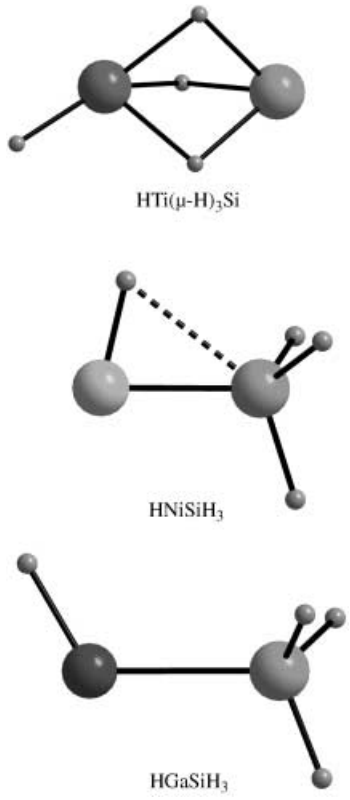

Figure 8. Structures of $MSiH_4$ molecules (M = Ti, Ni, Ga).

structures vary significantly. While $TiSiH_4$ features three Ti-H-Si bridges,[9] both $NiSiH_4$ and $GaSiH_4$ [8] exhibit only terminal Si–H and M–H bonds. $HNiSiH_3$ has the qualitative appearance of a transition state on the way to an insertion that starts with a metal atom which is coordinated side-on to an Si–H bond. It is possible that the transition state on the way to $HGaSiH_3$ formation has a comparable structure. The difference in structures is also caused by differences in electronegativity. An extreme description of the bonding in $HTi(\mu\text{-}H)_3Si$ is as a HTi^+ ion bound to an SiH_3^- ion. The electronegativities of Ni and Si, and also of Ga and Si, are not very different, and thus a direct covalent bond can be established. The hard–soft concept is also applicable.

Acknowledgement

The financial support of the Deutsche Forschungsgemeinschaft and the Fonds der Chemischen Industrie is gratefully acknowledged.

[1] S.-C. Chang, R. H. Hauge, W. E. Billups, J. L. Margrave, Z. H. Kafafi, *Inorg. Chem.* **1988**, *27*, 205.
[2] H. Burghgraef, A. P. J. Jansen, R. A. van Santen, *J. Chem. Phys.* **1993**, *98*, 8810.
[3] M. R. A. Blomberg, P. E. M. Siegbahn, U. Nagashima, J. Wennerberg, *J. Am. Chem. Soc.* **1991**, *113*, 424.
[4] See, for example: a) S. Sakaki, B. Biswas, M. Sugimoto, *Dalton Trans.* **1997**, 803; b) M-D. Su, S.-Y. Chu, *Inorg. Chem.* **1998**, *37*, 3400.
[5] K. Koszinowksi, D. Schröder, H. Schwarz, *J. Phys. Chem. A* **2003**, *107*, 4999.
[6] H.-J. Himmel, T. M. Greene, A. J. Downs, L. Andrews, *Organometallics* **2000**, *19*, 1060.
[7] B. Gaertner, H.-J. Himmel, *Angew. Chem.* **2002**, *114*, 1602; *Angew. Chem. Int. Ed.* **2002**, *41*, 1538.
[8] B. Gaertner, H.-J. Himmel, V. A. Macrae, A. J. Downs, T. M. Greene, *Chem. Eur. J.* **2004**, *10*, in press .
[9] A. Bihlmeier, T. M. Greene, H.-J. Himmel, *Organometallics* **2004**, *23*, in press.
[10] B. Gaertner, H.-J. Himmel, V. A. Macrae, J. A. J. Pardoe, P. G. Randall, A. J. Downs, unpublished results.
[11] H. Haberlandt, F. Ritschl, G. Pacchioni, *J. Phys. Chem.* **1991**, *95*, 4795.
[12] L. H. Dubois, B. R. Zegarski, *Surf. Sci.* **1988**, *204*, 113.
[13] See, for example: H.-J. Himmel, A. J. Downs, T. M. Greene, *Chem. Rev.* **2002**, *102*, 4191.
[14] R. Ahlrichs, M. Bär, M. Häser, H. Horn, C. Kölmel, *Chem. Phys. Lett.* **1989**, *162*, 165; K. Eichkorn, O. Treutler, H. Öhm, M. Häser, R. Ahlrichs, *Chem. Phys. Lett.* **1995**, *240*, 283; K. Eichkorn, O. Treutler, H. Öhm, M. Häser, R. Ahlrichs, *Chem. Phys. Lett.* **1995**, *242*, 652; K. Eichkorn, F. Weigend, O. Treutler, R. Ahlrichs, *Theor. Chem. Acc.* **1997**, *97*, 119; F. Weigend, M. Häser, *Theor. Chem. Acc.* **1997**, *97*, 331; F. Weigend, M. Häser, H. Patzelt, R. Ahlrichs, *Chem. Phys. Lett.* **1998**, *294*, 143.
[15] a) L. Manceron, M. E. Alikhani, H. A. Joly, *Chem. Phys.* **1998**, *228*, 73; b) L. Andrews, A. Citra, G. V. Chertihin, W. D. Bare, M. Neurock, *J. Phys. Chem. A* **1998**, *102*, 2561.
[16] a) R. L. DeKock, *Inorg. Chem.* **1971**, *10*, 1205; b) H. A. Joly, L. Manceron, *Chem. Phys.* **1998**, *226*, 61; c) M. Zhou, L. Andrews, *J. Am. Chem. Soc.* **1998**, *120*, 11499.
[17] D. M. Mann, H. P. Braida, *J. Chem. Phys.* **1971**, *55*, 84.
[18] M. Moskovits, J. E. Hulse, *J. Chem. Phys.* **1977**, *66*, 3988.
[19] In close proximity to the band at 1321.4 cm^{-1} is a band at 1320.5 cm^{-1} (not visible in the difference spectrum shown in Figure 7), the intensity of which is only slightly affected by photolysis. This band might arise from minor traces of diglyme from the preparation of SnD_4.
[20] H.-J. Himmel, L. Manceron, A. J. Downs, P. Pullumbi, *Angew. Chem.* **2002**, *114*, 829; *Angew. Chem. Int. Ed.* **2002**, *41*, 796.
[21] H.-J. Himmel, L. Manceron, A. J. Downs, P. Pullumbi, *J. Am. Chem. Soc.* **2002**, *124*, 4448.
[22] A. Köhn, H.-J. Himmel, B. Gaertner, *Chem. Eur. J.* **2003**, *9*, 3909.

Received: November 28, 2003

Published online: April 26, 2004

